FARMACIA, 2026, Vol. 74, 4

https://doi.org/10.31925/farmacia.2026.4.18 **ORIGINAL ARTICLE**

CELL AND DOSE-DEPENDENT ATTENUATION OF ATORVASTATIN ON LPS-ASSOCIATED TNF-α EXPRESSION AND THE ASSOCIATED TUMOR GROWTH INDUCTION IN BREAST CANCER CELLS

NADA ALMUTAIRI, NOJOOD ALTWAIJRY, SEEMA ZARGAR *

Department of Biochemistry, College of Science, King Saud University, PO Box 22452, Riyadh 11451, Saudi Arabia

**corresponding author: szargar@ksu.edu.sa*

Manuscript received: May 2026

Abstract

Chronic inflammation contributes to breast cancer progression through cytokine effects on tumor growth. Tumor necrosis factor- alpha (TNF-α) is a key inflammatory mediator implicated in breast cancer subtypes. Atorvastatin (ATO), beyond its lipid-lowering effects, has been reported to exert anti-inflammatory and anti-tumor properties. We investigated the effects of the ATO on TNF-α expression, secretion, and growth in MCF-7 and MDA-MB-231 breast cancer cells in response to lipopolysaccharide (LPS) stimulation. Treatments used were LPS 10 µg/mL) and ATO (0 - 9 µM), alone or combined. The antiproliferative effects of ATO were assessed by MTT and RTCA analysis. TNF-α mRNA expression and secretion levels were quantified by qPCR using TaqMan probes and by a Luminex immunoassay. ATO reduced the LPS-induced cell proliferation. ATO also lowered TNF-α gene expression relative to LPS-treated cells, although LPS-induced upregulation of TNF-α expression in MCF-7 cells did not reach statistical significance. In MDA-MB-231 cells, the effects of ATO were less pronounced, supporting a cell type- and dose-dependent pleiotropic anti-inflammatory action of ATO in breast cancer.

Rezumat

Inflamația cronică determină progresia cancerului mamar prin efectele citokinelor asupra creșterii tumorale. Factorul de necroză tumorală alfa (TNF-α) este un mediator inflamator esențial, implicat în diferite subtipuri de cancer mamar. Atorvastatina (ATO), dincolo de efectele sale hipolipemiante, a fost raportată ca având proprietăți antiinflamatoare și antitumorale. Au fost investigate efectele atorvastatinei asupra expresiei TNF-α și asupra proliferării celulare pe liniile de cancer mamar MCF-7 și MDA-MB-231, după stimularea cu lipopolizaharide (LPS). Dozele utilizate au fost LPS 10 µg/mL și ATO 0 - 9 µM, administrate individual sau în combinație. Efectele antiproliferative ale atorvastatinei au fost evaluate prin analize MTT și RTCA. Expresia ARNm și valorile TNF-α au fost cuantificate prin qPCR, utilizând sonde TaqMan, și printr-un imunotest Luminex. Atorvastatina a redus proliferarea celulară indusă de LPS. De asemenea, ATO a diminuat expresia genei TNF-α comparativ cu celulele tratate doar cu LPS, deși creșterea expresiei TNF-α indusă de LPS în celulele MCF-7 nu a atins pragul de semnificație statistică. În celulele MDA-MB-231, efectele atorvastatinei au fost mai puțin pronunțate, susținând o acțiune antiinflamatoare pleiotropă, în funcție de tipul celular și de doză.

Keywords: atorvastatin, LPS, TNF-α, drug repurposing, cytokines, pleiotropy, breast cancer

Introduction

Despite significant advancements in cancer research, cancers remain a challenge to treat due to issues like metastasis, recurrence, and drug resistance. Breast cancer, the most prevalent cancer among women worldwide, is driven by genetic and epigenetic alterations within the tumor microenvironment (TME). Inflammation, mediated by these alterations in pro-inflammatory cytokines, plays a crucial role in disease progression. Additionally, metabolic reprogramming of cancer cells and the TME facilitates tumor progression. Hence, targeting the TME by drugs that affect metabolism could offer new anti-cancer therapeutic strategies. Tumor necrosis factor-alpha (TNF-α), an essential pro-inflammatory cytokine, is abundant in the TME of breast cancer patients (1). It is secreted by various stromal cells, predominantly tumor-associated macrophages, and by the cancer cells.

The mevalonate pathway is essential for cholesterol production. Products of this pathway have been shown to promote migration, proliferation, and differentiation of breast cancer cells. Statins are approved drugs for cholesterol-lowering action (2). They inhibit the rate-limiting enzyme, 3-hydroxy-3-methylglutaryl-coenzyme A reductase (HMG-CoA reductase), of the mevalonate pathway. Lipophilic statins, including atorvastatin (ATO) and simvastatin, have been reported to inhibit growth and even induce cancer cell death (3). Cancer cells rely on anaerobic glycolysis for energy production even in the presence of adequate oxygen. This metabolic adaptation, commonly known as the Warburg effect, supports the energy demands of the TME. Because the mevalonate pathway is important in cellular

bioenergetics, statins, including ATO, have been proposed to indirectly modulate this energy demand of cancer cells in addition to their cholesterol-lowering action (3). However, the concentrations needed to produce these pleiotropic anti-cancer effects in the laboratory are much higher than the levels of ATO that reach the bloodstream in patients taking standard oral doses (10 - 80 mg/day). The oral bioavailability in patients taking ATO typically remains in the micromolar range (3-5). To bridge this gap, we used ATO concentrations ranging from 0.3 to 9 μM, with or without LPS, to enhance the overall anti-proliferative and anti-inflammatory effects against two breast cancer cell lines in this study.

Statins may suppress cancer cell proliferation by inducing cell cycle arrest (6-7). They may also modulate the immune response in breast cancer patients, but clinical data on this is limited (8). Simvastatin was found to inhibit the mevalonate pathway, which is involved in the synthesis of the mitochondrial electron carrier coenzyme Q10 (CoQ10), as well as other bioenergetic substrates (6). The use of statins in combination with trastuzumab lowered the cardiotoxicity of trastuzumab-based therapy in HER2-positive breast cancers (9). Inflammation contributes to various stages of carcinogenesis, from genomic instability to metastasis (10). However, little is known about the effect of statins on inflammation-associated cancers. To address this gap, we aimed to investigate the effects of ATO on LPS-induced breast cancer cell lines to explore whether it has a pleiotropic role with respect to TNF-α-driven inflammation in breast cancer. Temporally distinct parallel observations of TNF-α expression and secretion alongside cell proliferation are important for identifying the role of new therapeutic agents. This may provide new insights into its role in potential intervention pathways for inflammatory breast cancer. Examining the effect of ATO as an anti-inflammatory agent in breast cancer cells may provide insight into TNF-α-driven inflammatory responses and growth modulation. Such findings could support the rationale for combining ATO with other anti-cancer agents to improve the pleiotropic efficacy at clinically relevant concentrations.

LPS, a bacterial cell wall component, has been shown to exert diverse effects on the growth and inflammatory signaling of cancer cells. Evidence from animal models suggests that inflammation promotes genomic instability/DNA mutations, particularly through reactive oxygen species produced by activated inflammatory cells and inflammatory cytokines. DNA damage, in turn, exacerbates inflammation and promotes tumorigenesis. LPS-TLR4 signaling was associated with activation of the ERK and p38 MAPK pathways, which promoted cancer cell proliferation (11). In the inflammatory TME, immune cells such as monocytes and T cells encounter and respond to abnormal signals from the tumor by producing inflammatory mediators such as TNF-α. TNF-α is the most efficient target for modulating the inflammatory microenvironment for cancer therapy (12). Key cytokine signaling pathways, such as TNF-α, can promote cancer growth and suppress anti-tumor immunity, thereby reducing the effectiveness of chemotherapy (13). Inflammatory cytokines and death-inducing cytokines are produced by cancer cells themselves or by immune cells in a paracrine manner (13). At the dissemination stage, inflammatory cytokines increase the invasive capacity of malignant cells through upregulated expression (14) and contribute to metastasis by promoting the survival of circulating cancer cells (12). LPS, a potent inducer of inflammation, plays a prominent role in cytokine regulation and may contribute to breast cancer progression through TNF-α; hence, it was used to sensitize the cells.

This study aimed to investigate whether atorvastatin (ATO) attenuates LPS-induced changes in TNF-α gene expression, TNF-α protein secretion, and cell growth in luminal (MCF-7) and triple-negative (MDA-MB-231) breast cancer cell lines to evaluate the cell-type dependence of its pleiotropic anti-inflammatory action.

Materials and Methods

Cell culture and treatments

MCF-10A (CRL-10317, ATCC) MDA-MB-231 (HTB-26, ATCC) and MCF-7 (HTB-22, ATCC) breast cell lines were grown in Dulbecco's Modification of Eagle's Medium (DMEM) (Cat. No. 41966029, Invitrogen) supplemented with 10% FBS (Cat. No. F4135, Sigma), L-Glutamine (2 mM) (Cat. No. G7513-100ML, Sigma) and Penicillin/streptomycin (100 μg/mL) (Cat. No. 15140122, Thermo Fisher). The cells were maintained at 37°C in 5% CO_2 with around 300,000 cells/mL seeded in cell culture flasks for all experiments. The cells were treated with LPS (10 μg/mL) in the absence or presence of different doses of ATO (0 - 9 μM) (Sigma-Aldrich, Cat. No. PHR1422-1G, Sintra, Portugal). Each experiment was carried out at least three times to obtain statistically significant results. For all experiments, cells treated only with DMSO were used as a control. The final DMSO concentration used in all treatments and controls was 0.1% (v/v); the same final concentration was used to dissolve the drugs. The final concentration of DMSO was maintained at 0.1% (v/v) in all treatments. LPS and ATO were added simultaneously (co-treatment) for all combination groups. Cells were exposed to treatments for 24 h prior to the MTT assay to determine intrinsic TNF-α gene expression levels. Cell culture supernatants were collected after 48 h for Luminex analysis to measure secreted TNF-α levels. RTCA growth

was monitored continuously for up to 72 h following the treatments.

Proliferation assays

Cell proliferation was assessed using 3-(4,5-dimethylthiazol-2-yl)-2,5-diphenyltetrazolium bromide (MTT) assay to determine safe and effective drug concentrations. MCF-7 and MDA-MB-231 cells (1×10^3) were seeded in 96-well culture plates and incubated for 24 h with serum-free DMEM, followed by simultaneous treatments with 10 µg/mL LPS and/or varied concentrations of ATO. DMSO-treated cells served as controls. After treatment, MTT solution (5 mg/mL) was added, and the mixture was incubated for 3 h. Formazan crystals were dissolved, and absorbance was measured at 590 nm using an X-Mark microplate reader within one hour.

By using XCelligence real-time cell analysis (RTCA) cell proliferation assay (RTCA-DP version; Roche Diagnostics, Mannheim, Germany), MCF-7, MDA-MB-231, and MCF10A cells were grown in T-75 flasks to 60-80% confluency. To assess background electrical impedance, the 96-well electronic microtiter plate (E-plate) was first blanked with 50µl of DMEM in each well. Cells were then trypsinized and counted using a hemocytometer, then plated at 6,000-10,000 cells *per* well in a 96-well xCelligence E-plate with an additional 50 µL of DMEM (final well volume of 100 µL). Growth was monitored in real-time for up to 72 h, with impedance assessed at 15-minute intervals using the xCelligence Real-time Cell Analyzer (RTCA). Data exported from the xCelligence system were analyzed from each well. Cell growth results were presented as graphs showing the averages (± SD) from the experiments conducted (15).

Preparation of Total RNA Using TRI reagent and Taqman-based quantitative real-time PCR of TNF-α

Total RNA was extracted using TRI Reagent solution (Cat. No. T9424, Sigma) for the isolation of total RNA. Briefly, cells were lysed in the TRI reagent. After adding chloroform and centrifugation, the TRI reagent separated into two layers. The upper layer was aqueous and contained the RNA. The RNA was further purified by precipitation with isopropanol and subsequent ethanol washing. RNA purity was measured spectrophotometrically, and RNA with an O.D. ratio of A260/A280 > 1.8 (5 ng/µL) was used for cDNA preparation. cDNA from each treatment group was subjected to reverse transcription according to the manufacturer's protocol. Equal amounts of cDNA were subsequently used for qPCR amplification. with an oligo (dT) primer using Superscript II reverse transcriptase (Invitrogen) according to the manufacturer's protocol. Total cDNA was analyzed using quantitative real-time PCR (qRT-PCR) with TaqMan chemistry to measure mRNA expression levels, following the comparative Ct (threshold cycle) method as described previously (16). Expressions were analyzed using TaqMan probes obtained from Applied Biosystems. Reactions were performed in triplicate wells according to the manufacturer's instructions for the TaqMan predesigned gene expression assay for TNF-α (Cat. No. Hs00174128_m1). Amplification was carried out on an AB 7500 Fast instrument coupled with the TaqMan® Universal PCR Master Mix (Applied Biosystems) in fast cycling mode on a 2-step template. The reference gene was selected as 18S rRNA after performing a pilot validation of endogenous controls. Different experimental conditions were used, and constant Ct values were ensured for 18S rRNA. The cycling parameters were one cycle at 50°C for 2 minutes, followed by one cycle at 95°C and 60°C for 3 seconds, with 40 cycles of extension at 60°C for 30 seconds. Ct values were normalized to the endogenous control 18S rRNA gene (Assay ID: 4319413E). Relative expression of TNF-α was calculated by the $2^{-\Delta\Delta CT}$ method using 18S rRNA as the endogenous reference gene for all qPCR data reported in this study.

TNF-α cytokine quantification in cell supernatants by Luminex Multiplex Immunoassay

TNF-αlevels in cell culture supernatants were quantified using a bead-based multiplex immunoassay (Millipore, Merck) according to the manufacturer's instructions. Briefly, culture supernatants were collected, centrifuged at 1,000 × g for 5 min to remove cellular debris, and stored at -80 °C until analysis. Samples were thawed and assayed in technical triplicate. Magnetic capture beads specific for human TNF-α were incubated in a 96-well plate at room temperature with continuous shaking, along with standards, controls, and samples. Plates were washed and incubated with biotinylated detection antibodies, followed by streptavidin-phycoerythrin. Beads were then washed and resuspended in assay buffer before acquisition. Data were acquired using a Luminex LX100/LX200 system, and median fluorescence intensity (MFI) values were recorded. TNF-α concentrations were calculated from standard curves generated using a five-parameter logistic (5-PL) weighted regression model. TNF-α concentrations were expressed as pg/mL. Quality control samples and bead counts ≥ 50 *per* analyte were used to ensure assay reliability.

Statistical Analysis

The data were expressed as mean ± standard deviation and analyzed using Prism v.7.3 (GraphPad Inc., La Jolla, CA, USA). The groups were analyzed relative to the DMSO control using one-way analysis of variance (ANOVA), followed by Tukey's multiple comparisons test at a 95% confidence level. A p-value ≤ 0.05 was considered significant.

Results and Discussion

Effect of LPS and ATO on cell proliferation

LPS treatment significantly increased cell optical density compared with control in the MCF-7 cell line, confirming its robust stimulatory effect on cancer growth. ATO treatment alone did not significantly alter optical density relative to control, indicating a lack of intrinsic stimulatory activity. Importantly, co-treatment with ATO and LPS reduced LPS-induced optical density across all ATO treatments ($p < 0.0001$ to $p < 0.0057$) compared to control, demonstrating a protective effect by attenuating LPS-mediated stimulation (Figure 1).

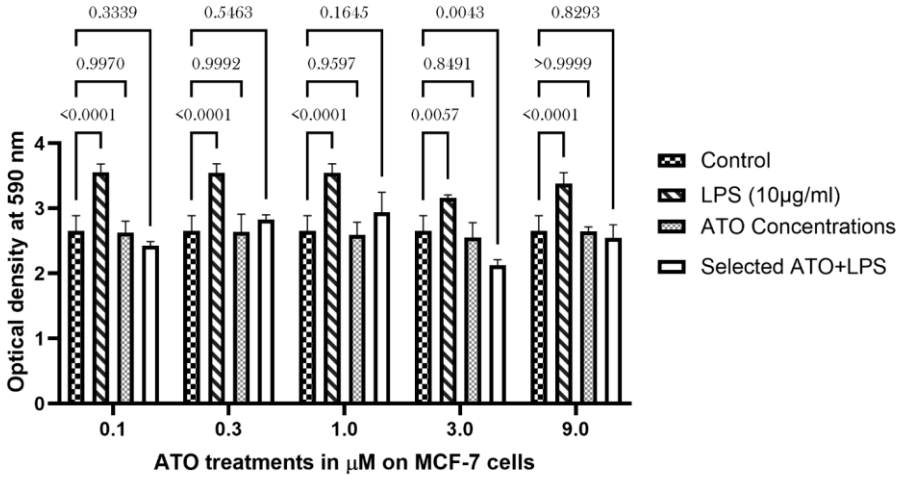

Figure 1.

Effect of varying concentrations of atorvastatin (ATO) on LPS-induced cell proliferation in the MCF-7 cell line, measured at 590 nm by MTT assay. Cells were treated with increasing concentrations of ATO (0.1, 0.3, 1.0, 3.0, and 9.0 μM) in the absence or presence of lipopolysaccharide (LPS, 10 μg/mL) and compared with DMSO-treated controls. ATO attenuates LPS-induced proliferation ($p < 0.0001$). The addition of ATO, alone or in combination, reversed it to non-significant levels at all concentrations; p-values are indicated above each panel.

LPS treatment (10 μg/mL) also significantly increased optical density in MDA-MB-231 cells compared with DMSO-treated control cells across all tested concentrations ($p < 0.0001$), confirming a robust stimulatory/inflammatory response in this cell line as well. Treatment with ATO alone resulted in optical density values that were comparable to the control group across the concentration range, with no statistically significant differences observed between control and ATO-treated cells. Importantly, co-treatment with ATO and LPS significantly reduced the LPS-induced increase in optical density. This protective effect of ATO was evident at lower concentrations (0.1-1.0 μM), where ATO + LPS groups showed a significant decrease compared with LPS alone ($p = 0.0004$ at 0.3 μM and $p = 0.0028$ at 1.0 μM). At higher concentrations (3.0 and 9.0 μM), ATO + LPS treatment continued to show a downward trend relative to LPS alone, although the differences did not reach statistical significance ($p = 0.0861$ and $p = 0.3092$, respectively). Overall, these results demonstrate that LPS strongly stimulates the measured response in MDA-MB-231 cells, whereas ATO alone is non-stimulatory but shows significantly slower growth when compared to the control. Notably, ATO attenuates LPS-induced activity, particularly at lower concentrations, supporting a protective, anti-inflammatory role of ATO in this triple-negative breast cancer cell line (Figure 2).

Real-time cell analysis was tested during LPS induction with ATO treatments at 0.3 and 3 μM in both breast cancer cells and the normal cell line MCF-10A. LPS alone caused a mild increase in proliferation, as evidenced by an elevated cell index relative to the DMSO control in cancer cell lines, but not in normal breast MCF-10A cells. (Figure 3). LPS produced a mild increase in cell index relative to the DMSO control in the cancer cell lines but not in the non-tumorigenic MCF-10A cell line. ATO treatment led to a dose-dependent reduction in cell index generated using the xCELLigence RTCA system, following LPS and ATO treatments. ATO, alone and in combination at all concentrations, showed a dose-dependent reduction in cell proliferation, attributed to its lipid-lowering action in these cells, observed at approximately 19-20 h after treatment.

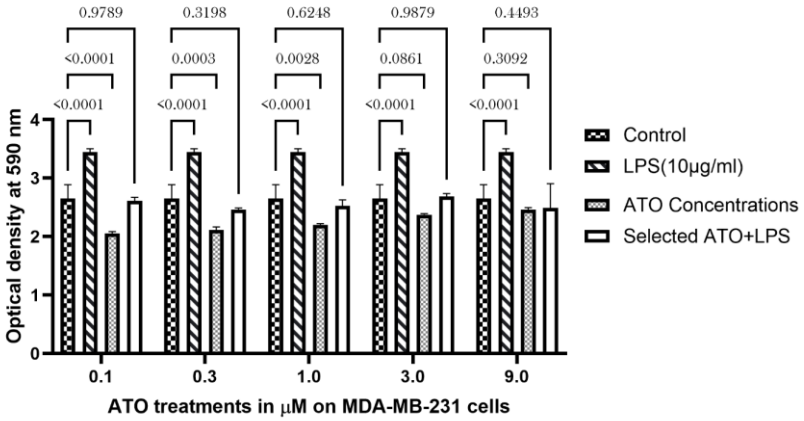

Figure 2.

Effect of varying concentrations of atorvastatin (ATO) on LPS-induced cell proliferation in the MDA-MB-231 cell line, measured at 590 nm by MTT assay. Cells were treated with increasing concentrations of ATO (0.1, 0.3, 1.0, 3.0, and 9.0 μM) in the absence or presence of lipopolysaccharide (LPS, 10 μg/mL) and compared with DMSO-treated controls. LPS induced significant proliferation ($p < 0.0001$), and ATO attenuated LPS-induced proliferative activity across all concentrations. ATO alone at 0.1 and 0.3 μM reduced cell proliferation below the control.

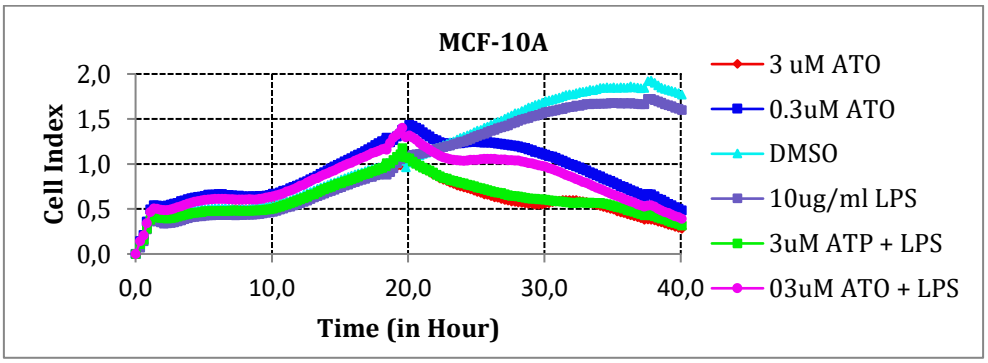

Figure 3.

Real-time cell analysis (RTCA) cell proliferation curve (cell index vs time, hours) for MCF-10A normal breast cells treated with vehicle control (DMSO), LPS (10 μg/mL), ATO (0.3 μM or 3 μM) alone, or the indicated ATO + LPS combinations. Data were displayed as mean ± SD from 3 technical replicates and were representative of 3 independent experiments; proliferation is expressed as a normalized cell index (CI). MCF-10A cell line was included here solely for a proliferation comparison with breast cancer cells and was not evaluated in the MTT, qPCR, or Luminex assays. LPS alone did not increase proliferation in normal breast MCF-10A cells, and ATO alone, as well as in combination with LPS, decreased proliferation at both selected concentrations ($p \leq 0.0001$).

Figure 4 depicts the real-time growth kinetics of MCF-7 cells under control conditions and following treatment with LPS, atorvastatin (ATO) at different concentrations, and combined ATO + LPS exposure. Cell index values increased progressively over time in control cells, reflecting sustained proliferation throughout the experimental period. LPS treatment resulted in a consistently higher growth trajectory compared with control, indicating a stimulatory effect on cell proliferation and survival. This increase became more pronounced at later time points, suggesting that inflammatory stimulation promotes continued cellular expansion in MCF-7 cells. In contrast, ATO treatment alone altered cell growth dynamics in a concentration-dependent manner. ATO treatment, alone and in combination, significantly reduced cell growth dynamics in a dose-dependent manner. The lower concentration of 0.3 μM produced a growth curve that decreased moderately relative to LPS-treated and control cells throughout the monitoring period. In contrast, 3 μM ATO produced a considerable attenuation of the growth curve beginning at approximately 19-20 h post-treatment, indicating a reduction in net cell growth restricted to the 3 μM ATO concentration alone and in combination with LPS in MCF-7 cells (Figure 4).

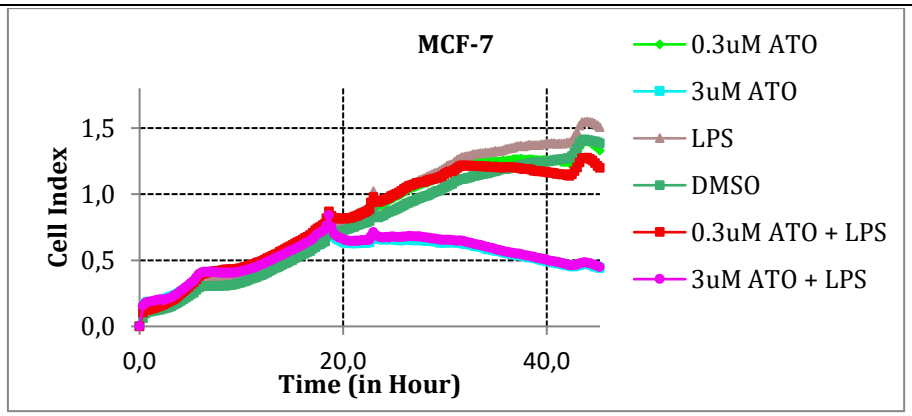

Figure 4.

Real-time cell analysis (RTCA) cell proliferation curve (cell index vs time, hours) for MCF-7 breast cancer cells treated with vehicle control (DMSO), LPS (10 µg/mL), ATO (0.3 µM and 3 µM) alone, or the indicated ATO + LPS combinations. Data were displayed as mean ± SD from 3 technical replicates and were representative of 3 independent experiments; proliferation is expressed as a normalized cell index (CI). 3 µM ATO and 3 µM ATO+LPS diverged from all other groups after 18-20 h, declining to the lowest cell index by 45 h (endpoint CI values compared by one-way ANOVA with Tukey's test; $p \leq 0.005$) (Colors indicate the treatment groups).

Figure 5 illustrates the real-time proliferation analysis across all treatments in MDA-MB-231 cells relative to DMSO control cells. LPS treatment moderately enhanced proliferation, while ATO treatment alone and in combination reduced growth in a concentration-dependent manner, with higher doses causing marked growth inhibition after treatment. Notably, co-treatment with ATO and LPS attenuated the LPS-induced increase in cell growth, resulting in a progressive decline in cell index. These findings indicate that ATO significantly suppresses LPS-induced cell proliferation and counteracts LPS-induced stimulation in the aggressive triple-negative cell line (Figure 5).

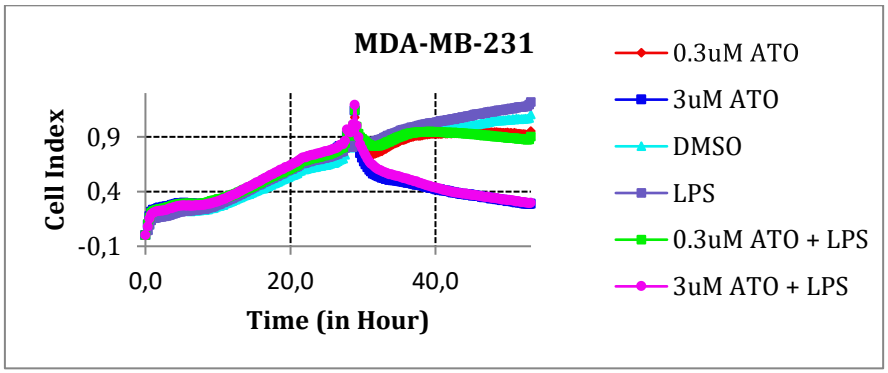

Figure 5.

Real-time cell analysis (RTCA) cell proliferation curve (cell index vs time, hours) for MDA-MB-231 breast cancer cells treated with vehicle control (DMSO), LPS (10 µg/mL), ATO (0.3 µM and 3 µM) alone, or the indicated ATO + LPS combinations. Data were displayed as mean ± SD from 3 technical replicates and were representative of 3 independent experiments; proliferation was expressed as a normalized cell index (CI). 3 µM ATO and 3 µM ATO+LPS diverged from all other groups after 28-30 h, declining to the lowest cell index by 55 h (endpoint values; CI compared by one-way ANOVA with Tukey's test, $p \leq 0.0005$) (Colors indicate the treatment groups).

Notably, co-treatment with ATO and LPS markedly modified the LPS-induced growth patterns in cells. While initial growth was comparable to that observed with LPS alone, the combined ATO + LPS groups demonstrated a clear divergence at later stages, with a pronounced reduction in cell index compared with LPS-treated cells. This effect suggests that ATO effectively counteracts LPS-mediated enhancement of cell growth in cancer cells, resulting in suppressed proliferation over time, supporting its protective and anti-inflammatory role in limiting inflammation-driven tumor cell growth. In contrast to the MCF-7 cell line, ATO treatment alone in the MDA-MB-231 cell line at 0.3 and 3 µM showed a progressive decline in cell index at approximately 29-30 h post-treatment, in a dose-dependent manner. This indicates that the growth-inhibitory effect of ATO in MDA-MB-231 cells is delayed. The growth-inhibitory effect of ATO was observed at a 10 h delay relative to MCF-7 cells. This result may be

attributed to the more aggressive and rapidly proliferating nature of the triple-negative MDA-MB-231 cell line.

Despite the advancements in cancer research, breast cancer remains challenging to treat due to issues like metastasis, recurrence, and drug resistance. LPS treatment induces TNF-α, which plays a dual role in facilitating tumor progression or directly mediating tumor cell killing. TNF-α increases the invasive capacity of tumor cells by altering the inflammatory cascade within the tumor. In the TME, it contributes to metastasis by promoting the survival of circulating tumor cells and may promote apoptosis under certain conditions (17). Cholesterol-lowering medications during the adjuvant endocrine therapies have played important roles in preventing breast cancer recurrence. The use of cholesterol-lowering medication in a double-blind study with 8,010 hormone receptor-positive breast cancer postmenopausal women improved survival and reduced recurrence (18). Understanding the intricate interplay between TNF-α's apoptotic potential and the tumor-promoting inflammation induced by LPS and ATO treatments is crucial for designing targeted therapies. This study aimed to investigate the impact of ATO treatment on TNF-α expression and cell proliferation in LPS-induced breast cancer cells. Previously, Li *et al*. (2017) demonstrated the effectiveness of 10 µg/ml LPS in breast cancer cells, and Hsieh *et al*. (2025) also used 10 µg/mL LPS in their studies across different cell lines to induce an inflammatory response (19-20). ATO was tested over a screening range (0-9 µM) to define a dose-response in the presence and absence of LPS in the two selected breast cancer cell lines. LPS increased cell index relative to the DMSO control in cancer cell lines, but not in the non-cancerous MCF-10A cell line, which showed a mild decrease. The MCF-10A cell line is non-tumorogenic and was used solely for proliferation comparison with breast cancer cells and was not evaluated in the MTT, qPCR, or Luminex assays. A previous study reported higher structural integrity in normal MCF-10A cells than in cancerous cell lines, resulting in differential responses that may explain the mild decrease in the RTCA profile (21). Antiproliferative effects of ATO-alone treatments in cell lines may be attributed to inhibition of HMG-CoA reductase, a rate-limiting enzyme in mevalonate synthesis (cholesterol biosynthesis). Pathway products such as dolichol, GGPP, and farnesyl pyrophosphate play important roles in both the S and G1 phases of the cell cycle (22). Importantly, in MCF-7 cells (Figure 4), the reduction in the growth curve by 3 µM ATO compared to the control is apparent at approximately 20 h post-treatment. In contrast, in MDA-MB-231 cells (Figure 5), the reduction was observed at approximately 30 h post-treatment. This 10 h difference in onset timing may reflect the distinctly different basal proliferation rates and intrinsic inflammatory signaling backgrounds of the two cell lines. A recent study reported differences between two cell lines in adherence, migration, and invasion behaviors (23). The MDA-MB-231 triple-negative cells appear to sustain growth and proliferation for a longer duration before the growth inhibitory effect of ATO becomes detectable. Additionally, it was reported that MDA-MB-231 cells exhibit prolonged growth and proliferation due to their ability to sustain growth, and this behavior is crucial for their anchorage-independent survival and metastasis (24-25). This showed that the anti-proliferative effect of ATO is cell-type- and concentration-dependent.

Effect of LPS and ATO on TNF-α gene expression and TNF-α protein expression

Next, we sought to test differences in the mRNA abundance of the TNF-α gene in LPS-induced MDA-MDB-231 and MCF-7 Breast Cancer cells to show that cell proliferation is associated with TNF-α-driven inflammation-associated cytotoxicity. Tumor necrosis factor α (TNF-α) plays a crucial role in initiating inflammatory responses. While TNF-α has been shown to induce cell death in certain types of cancer, in others it can also exhibit tumor-promoting effects, including stimulation of transformation, proliferation, angiogenesis, invasion, and metastasis. LPS induction in MCF-7 and MDA-MB-231 breast cancer cells increased TNF-α gene expression (Figure 6). LPS stimulation significantly upregulated TNF-α gene expression in MDA-MB-231 breast cancer cells but not in MCF-7 breast cancer cells, compared to their DMSO controls. All experiments were performed at least 3 times.

The results demonstrated that LPS-induced TNF-α is cell line-dependent and more pronounced in MDA-MB-231 cells. The TNF-α upregulation in cell lines was temporally distinct and parallel with the moderate increase in proliferation rates observed upon LPS induction. TNF-α mRNA expression in MCF-7 cells following treatment with LPS and increasing concentrations of ATO alone or in combination is shown in Figure 7. ATO treatment alone at 0.3, 1, 3, or 9 µM did not alter TNF-α mRNA levels relative to the control (ns), indicating that ATO alone does not induce TNF-α expression. Similarly, co-treatment with LPS and varied ATO concentrations (0.3, 3, and 9 µM) did not significantly modify the LPS-induced response. Notably, co-treatment with LPS and 1 µM ATO resulted in a marked and significant increase in TNF-α expression compared with the DMSO control ($p < 0.0001$), suggesting a concentration-specific spike in TNF-α transcription and a non-monotonic dose response (Figure 7).

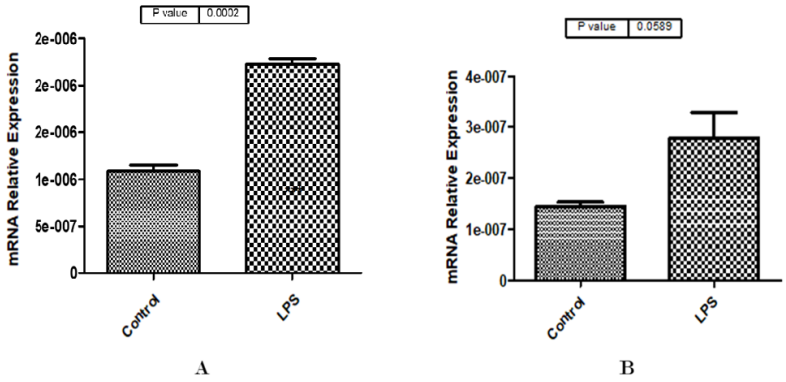

Figure 6.

Effect of LPS induction on TNF-α gene expression in breast cancer cell lines. LPS stimulation upregulated TNF-α gene expression in breast cancer cells. A: MDA-MB-231 cells were significantly upregulated ($p < 0.0002$ with LPS stimulation; B: MCF-7 cells showed non-significant upregulation in TNF-α by LPS-induction when compared to the DMSO control group $p \leq 0.0589$), n = 3 of three independent experiments.

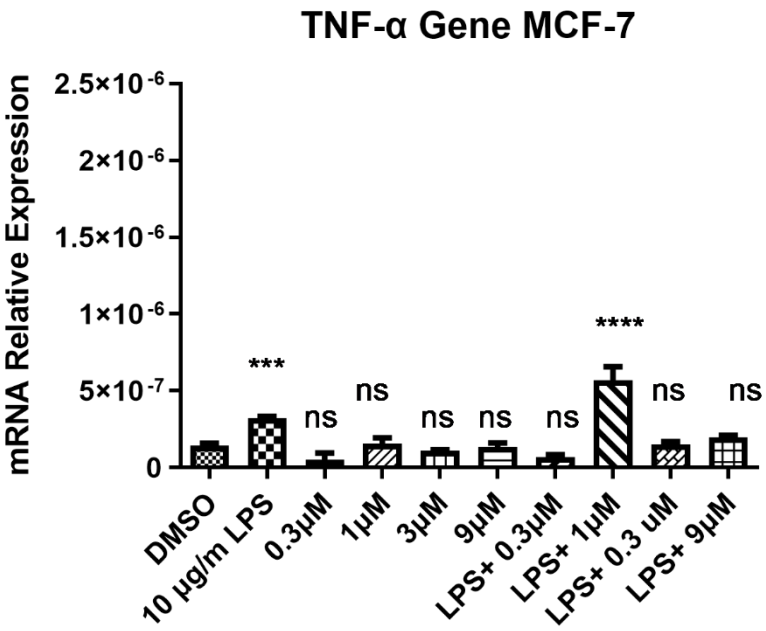

Figure 7.

Effect of varied concentrations of ATO on TNF-α induced by 10 µg/mL LPS in MCF-7 cells. 0.3 µM and 9 µM ATO downregulated inflammatory cytokine upregulation, but mid-treatment with 1µM ATO itself increased inflammatory cytokine levels, indicating dose-dependent mechanisms with respect to anti-inflammatory action in this cell line. Data are presented as mean ± SD. Statistical significance is indicated as ***$p < 0.001$, ****$p < 0.0001$; ns, not significant. *versus* the DMSO control.

Figure 8 shows TNF-α gene expression in MDA-MB-231 cells following treatment with LPS and ATO. The results showed that LPS significantly increased TNF-α expression compared with the control, whereas ATO alone reduced TNF-α levels. Co-treatment with ATO, however, did not significantly attenuate LPS-induced TNF-α expression and provided only partial protection. Although ATO significantly reduced basal TNF-α expression, it failed to fully attenuate LPS-induced TNF-α upregulation in MDA-MB-231 cells, suggesting cell-type–specific resistance to anti-inflammatory modulation. The aggressive and intrinsically inflammatory nature of triple-negative breast cancer cells, along with constitutive activation of inflammatory signaling pathways, may limit the capacity of ATO to suppress LPS-driven TNF-α transcription, resulting in only partial protection (Figure 8).

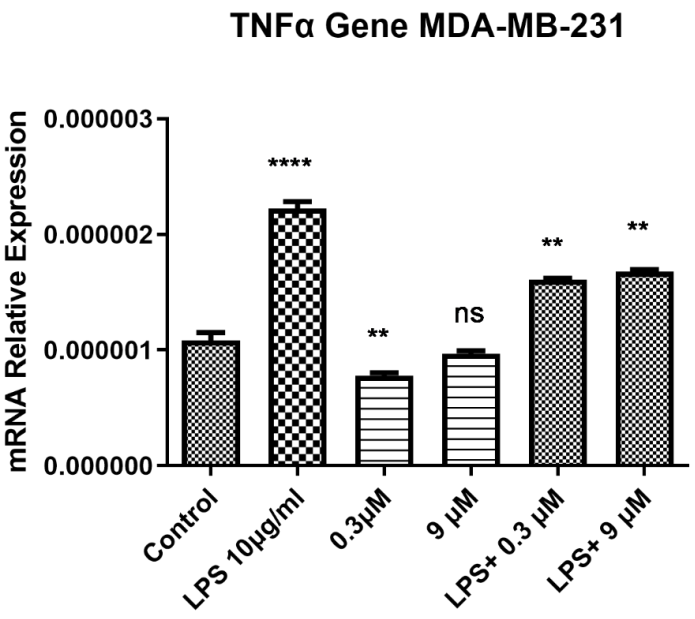

Figure 8.
Effect of varied concentrations of ATO on TNF-α induced by 10 µg/mL LPS in MDA-MB-231 cells. LPS significantly increased TNF-α expression, whereas ATO alone reduced basal TNF-α levels. Co-treatment with ATO partially reduced LPS-induced TNF-αexpression but did not fully suppress the inflammatory response. Data are shown as mean ± SD. Statistical significance is indicated as **$p < 0.01$, ****$p < 0.0001$; ns, not significant.

To test if Atorvastatin modulates LPS-associated TNF-α secretion in a cell line-dependent manner, we next sought to validate transcriptional changes in the tumor microenvironment. To validate the complement TNF-α transcript analysis, secreted TNF-α was quantified in conditioned media by Luminex multiplex immunoassay. TNF-αprotein levels measured in culture supernatants closely align with the observed TNF-α gene expression profile and cell growth behavior in MCF-7 cells. As shown in Figure 9, LPS treatment altered TNF-α secretion compared with the control. This finding is consistent with the corresponding TNF-α mRNA data, in which LPS induced only a moderate transcriptional upregulation. ATO treatment alone reduced TNF-α secretion, particularly at higher concentrations (9 µM), mirroring the absence of TNF-α gene induction under ATO-only conditions. This suppression at both the mRNA and protein levels by ATO treatment suggests that ATO may not rely solely on anti-inflammatory signaling via TNF-α in MCF-7 cells and instead exerts an anti-inflammatory effect through other mechanisms. Notably, co-treatment with ATO and LPS significantly reduced TNF-α protein secretion compared with LPS alone. This likely reflects post-transcriptional regulation of TNF-α secretion and highlights the capacity of MCF-7 cells to secrete TNF-α protein. TNF-α expression with ATO alone treatment at 9 µM and LPS treatment could represent an autocrine feedback loop in MCF-7 cells that promotes proliferation pathways (Figure 9).

In MDA-MB-231 cells, the basal TNF-α secretion was detectable in untreated control cells, reflecting the intrinsically inflammatory phenotype of this triple-negative breast cancer cell line. LPS treatment (10 µg/mL) significantly increased TNF-α secretion compared with control ($p < 0.01$), confirming a strong inflammatory response. ATO treatment alone at 0.3 and 9 µM resulted in a non-significant reduction in TNF-α secretion relative to control cells; however, these changes did not reach statistical significance, indicating limited suppression of basal cytokine release compared with the MCF-7 cell line, consistent with its aggressive nature. Co-treatment of ATO and LPS attenuated LPS-induced TNF-α secretion at 3 µM but not at 0.3 µM, indicating dose dependence (Figure 10).

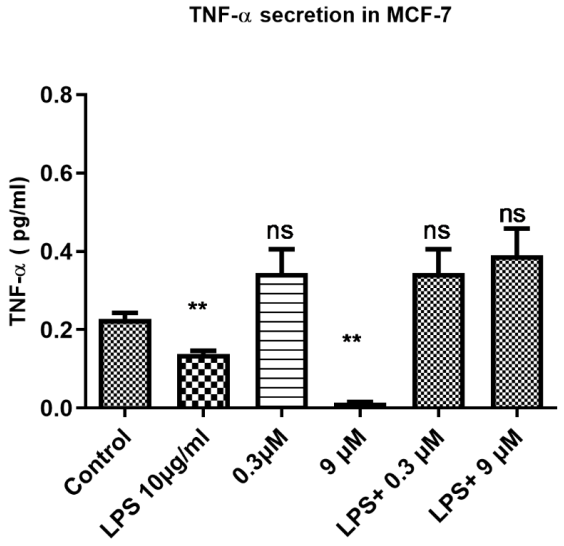

Figure 9.

TNF-α secretion in MCF-7 cells following treatment with lipopolysaccharide (LPS) and atorvastatin (ATO). Cells were treated with LPS (10 µg/mL), ATO alone (0.3 and 9 µM), or in combination with LPS. Secreted TNF-α levels in culture supernatants were quantified by a Luminex bead-based multiplex assay and expressed as pg/mL. Data are presented as mean ± SD. Statistical significance is indicated as **p < 0.01; ns, not significant when compared to control.

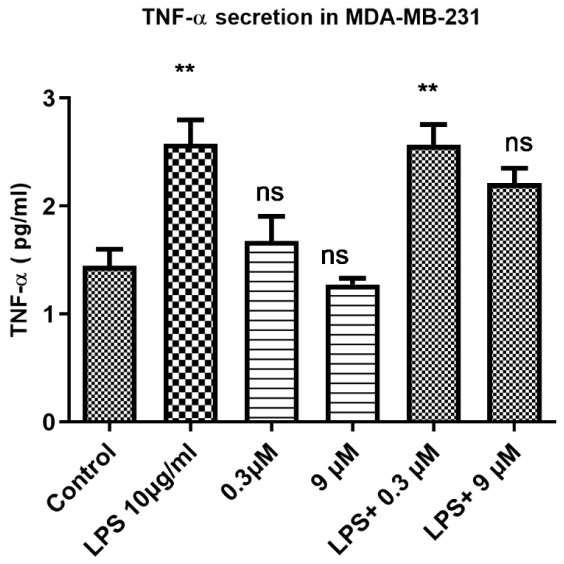

Figure 10.

TNF-α secretion in MDA-MB-231 cells following treatment with lipopolysaccharide (LPS) and atorvastatin (ATO). Cells were treated with LPS (10 µg/mL), ATO alone (0.3 and 9 µM), or in combination with LPS. Secreted TNF-αlevels in culture supernatants were quantified by a Luminex bead-based multiplex assay and expressed as pg/mL. Data are presented as mean ± SD. Statistical significance is indicated as **p < 0.01; ns, not significant when compared to control.

TNF-α is a multifunctional pro-inflammatory cytokine that plays a central role in systemic inflammation. It influences nearly all human organs and participates in numerous biological functions, including cell growth and differentiation, programmed cell death, lipid metabolism, and blood coagulation. In addition, TNF-α is a key contributor to the development of many diseases and biological processes (26-27). During inflammatory processes, immune cells in the TME encounter and respond to abnormal tumor-derived signals by producing inflammatory mediators such as TNF-α. By integrating gene expression, secretion, and real-time proliferation analysis, we demonstrate that the inflammatory

response to LPS is modulated by ATO and is cell-type- and dose-dependent. Our results are consistent with previous studies that reported LPS-induced activation of TLR4 signaling promotes cancer cell proliferation. LPS-TLR4 signaling has been previously associated with activation of the ERK and p38 MAPK signaling pathways, which promote cancer cell proliferation (11, 28) and cell migration and invasion in breast cancer cells (29). The anti-proliferative effects of ATO could result from inhibition of the mevalonate pathway and the Warburg effect (a hallmark of cancer) in cancer cells. LPS induction in MCF-7 and MDA-MB-231 breast cancer cells increased TNF-α gene expression. A previous study reported that LPS activates inflammasomes in cancer cells through NF-κB and promotes metastasis through glycolysis enhanced by the NF-κB/Snail/HK3 signaling pathway in colorectal cancer (CRC), and reported the protective effect of metformin on LPS-activated inflammasomes (30). Targeting TNF-α or its downstream metabolic effects (Warburg effect) with ATO could provide a strategy to limit LPS/TLR4-driven inflammatory signaling in breast cancer cells, particularly in aggressive triple-negative models (31). In the MCF-7 cell line, ATO alone at 9 μM and LPS treatment reduced TNF-α secretion in culture supernatants below control levels, suggesting an autocrine feedback loop that promotes proliferation pathways in cancer cells. Autocrine feedback signaling is defined as the production and secretion of a mediator (*i.e.*, a cytokine) by a cell, followed by its binding to receptors on the surface of the secreting cell to initiate signaling. Such an autocrine feedback loop has already been established in cancer cells for TGF-β and TNF-α (32). Notably, the pattern of TNF-α protein secretion in the combination-treated group and the trend observed in the growth-curve data in MCF-7 cells were obtained at different time points (48 h *vs* up to 72 h) and are interpreted here as temporally distinct, associative observations rather than proven correlations. This further supports an autocrine feedback loop in activating cell-proliferation signaling, as previous studies have reported TNF-α as a pleiotropic cytokine that activates distinct downstream signaling pathways, leading to cell death or survival (33).

Also, in MCF-7 cells, ATO treatment alone at 0.3, 1, 3, or 9 μM did not alter TNF-α mRNA levels relative to the control (ns), indicating that ATO alone does not induce TNF-α expression. Similarly, co-treatment with LPS and ATO concentrations (0.3, 3, and 9 μM) did not significantly modify the LPS-induced response. Notably, co-treatment with LPS and 1 μM ATO resulted in a marked and significant increase in TNF-α expression compared to the DMSO control ($p < 0.0001$), suggesting a U-shaped concentration-specific spike in TNF-α transcription and a non-monotonic dose response. This finding reveals a biphasic dose-response curve at the mRNA level and the distinct decoupling between gene transcription and functional protein secretion in the MCF-7 cell line, as transcriptional induction did not uniformly translate into increased TNF-α secretion. Upon LPS induction, the reduced secretion of TNF-α may be attributed to a concentration-dependent, transient interruption of isoprenoid synthesis in the mevalonate pathway. Interrupted isoprenoid biosynthesis leads to depletion of critical lipid intermediates, such as farnesyl pyrophosphate and geranylgeranyl pyrophosphate (GGPP), which directly disrupts the secretion of inflammatory cytokines (34). Despite the increased mRNA level, secreted TNF-α remained low and was completely normalized to baseline by ATO treatment. Consistent with our study, post-transcriptional/secretory regulation specific to luminal estrogen receptor-positive (ER+) MCF-7 breast cancer cells was reported to have comparatively low constitutive cytokine-secretory capacity relative to triple-negative lines (35-36).

Overall, these results highlight a differential and context-dependent role of ATO in modulating TNF-α-associated signaling in breast cancer. The ability of the ATO to suppress TNF-α gene expression and secretion, along with inhibiting growth responses in breast cancer cells, underscores the complexity of targeting TNF-α in luminal and TNBCs. Recent evidence shows that the cytokines and other inflammatory molecules play a role in the development of new and potential anticancer therapies (37). The study reported that blocking IL-1β with atorvastatin could resolve inflammation regardless of whether the cytokine is released from the cell or its precursor is cleaved (22). Multiple studies have highlighted the contribution of several transcription factors, including nuclear factor of activated T cells (NFAT) and NF-κB, in regulating the TNF-α promoter, providing a mechanistic explanation for the rapid induction of TNF-α expression following diverse stimuli (23). Foundational work using human TNF-α transgenic mouse models demonstrated that substitution of the native TNF-α 3′ untranslated region (UTR) with the β-globin mRNA 3′ UTR was sufficient to induce excessive TNF-α expression and cause tissue-specific inflammatory disease, regardless of the promoter driving the transgene (24). Subsequent studies showed that the TNF-α promoter exhibits constitutive activity in several cell lines, including HeLa, NIH3T3, and L929 cells. However, incorporation of the TNF-α 3′ UTR markedly suppressed reporter gene expression in HeLa and NIH3T3 cells, while this inhibitory effect was absent in L929 cells, underscoring the cell-type-specific regulatory function of the TNFα 3′ UTR (34). The functional relevance of these TNF-α inflammatory patterns was further supported by the growth curve data. In MCF 7 cells, limited TNF-α secretion was associated with

minimal changes in growth kinetics upon LPS stimulation, consistent with the low constitutive cytokine-secretory capacity of luminal breast cancer. Conversely, in MDA-MB-231 cells, elevated TNF-α secretion was temporally distinct and parallel to altered growth behavior, supporting the role of TNF-α as an autocrine mediator of tumor-associated inflammation in TNBC (24).

Limitations of this study

TNF-α secretion levels in cell culture supernatants from MCF-7 cells require a time-course evaluation in future studies. Non-monotonic responses described in this study may reflect concentration-dependent shifts in mevalonate pathway intermediates and need further evaluation. Other cytokines and mediators of inflammation may also be altered by treatments and, hence, should be evaluated in future studies, as they can provide essential mechanisms of ATO attenuation and further support the anti-inflammatory effect of ATO.

Conclusions

This study suggested that LPS exposure in the MCF-7 cell line increased TNF-α mRNA at 24 h, while the corresponding secreted TNF-α in cell culture supernatants at 48 h decreased. In contrast, the MDA-MB-231 cells showed increased TNF-α secretion in response to increased mRNA levels. Also, ATO treatments in combination with LPS in MCF-7 cells showed a biphasic, non-monotonic feedback response across the tested concentrations. ATO alone treatments in MDA-MB-231 cells showed limited suppression of basal TNF-α secretion compared with the MCF-7 cell line, which may indicate its aggressive nature and constitutive inflammatory phenotype, not directly tested in this study. Together, these findings suggest that atorvastatin's anti-inflammatory effects on TNF-α mRNA expression and secretion may be cell line- and dose-dependent. The study findings support the pleiotropic anti-inflammatory potential of ATO in breast cancer and warrant further investigation with matched time points.

Acknowledgement

The authors extend their appreciation to the Ongoing Research Funding Program (ORF-2026-1685) at King Saud University, Riyadh, Saudi Arabia, for funding this research.

Funding

The authors extend their appreciation to the Ongoing Research Funding Program (ORF-2026-1685) at King Saud University, Riyadh, Saudi Arabia, for funding this research.

Availability of data and materials

The data generated in the present study are included in the figures and/or tables of this article.

Ethics approval and consent to participate

Not applicable.

AI use disclosure

Not applicable.

Conflict of interest

The authors declare no conflict of interest.

References

1. Yang W, Bai Y, Xiong Y, Zhang J, Chen S, Zheng X, et al. Potentiating the antitumour response of CD8+ T cells by modulating cholesterol metabolism. Nature. 2016;531(7596):651-655.
2. Juarez D, Fruman DA. Targeting the mevalonate pathway in cancer. Trends Cancer. 2021;7(6):525-540.
3. Clim A, Mărănducă MA, Pinzariu AC, Cozma CT, Șerban DN, Șerban IL, et al. Oxidative stress: marker of endothelial dysfunction in experimental models of rats with hyperhomocysteinemia. Farmacia. 2024;72(6):1308-1316.
4. Lennernäs H. Clinical pharmacokinetics of atorvastatin. Clin Pharmacokinet. 2003;42(13):1141-1160.
5. Corsello SM, Nagari RT, Spangler RD, Rossen J, Kocak M, Bryan JG, et al. Discovering the anti-cancer potential of non-oncology drugs by systematic viability profiling. Nat Cancer. 2020;1(2):235-248.
6. Kuzyk CL, Anderson CC, Roede JR. Simvastatin induces delayed apoptosis through disruption of glycolysis and mitochondrial impairment in neuroblastoma cells. Clin Transl Sci. 2020;13(3):563-572.
7. Osmak M. Statins and cancer: current and future prospects. Cancer Lett. 2012;324(1):1-12.
8. Kim J, Choi EA, Han YE, Lee JW, Kim YS, Kim Y, et al. Association between statin use and all-cause mortality in cancer survivors, based on the Korean health insurance service between 2002 and 2015. Nutr Metab Cardiovasc Dis. 2020;30(3):434-440.
9. Calvillo-Argüelles O, Abdel-Qadir H, Michalowska M, Billia F, Suntheralingam S, Amir E, et al. Cardioprotective effect of statins in patients with HER2-positive breast cancer receiving trastuzumab therapy. Can J Cardiol. 2019;35(2):153-159.
10. Wen Y, Zhu Y, Zhang C, Yang X, Gao Y, Li M, et al. Chronic inflammation, cancer development and immunotherapy. Front Pharmacol. 2022;13:1040163.
11. Zu Y, Ping W, Deng T, Zhang N, Fu X, Sun W. Lipopolysaccharide-induced toll-like receptor 4 signaling in esophageal squamous cell carcinoma promotes tumor proliferation and regulates inflammatory cytokines expression. Dis Esophagus. 2017;30(2):1-8.
12. Mantovani A, Allavena P, Sica A, Balkwill F. Cancer-related inflammation. Nature. 2008;454(7203):436-444.

13. Lan T, Chen L, Wei X. Inflammatory cytokines in cancer: comprehensive understanding and clinical progress in gene therapy. Cells. 2021;10(1):100.
14. Pradhan R, Kundu A, Kundu CN. The cytokines in tumor microenvironment: from cancer initiation-elongation-progression to metastatic outgrowth. Crit Rev Oncol Hematol. 2024;196:104311.
15. Stefanowicz-Hajduk J, Ochocka JR. Real-time cell analysis system in cytotoxicity applications: usefulness and comparison with tetrazolium salt assays. Toxicol Rep. 2020;7:335-344.
16. Livak KJ, Schmittgen TD. Analyzing real-time PCR data by the comparative CT method. Nat Protoc. 2008;3(6):1101-1108.
17. Ben-Baruch A. The tumor-promoting flow of cells into, within and out of the tumor site: regulation by the inflammatory axis of TNFα and chemokines. Cancer Microenviron. 2012;5(2):151-164.
18. Borgquist S, Giobbie-Hurder A, Ahern TP, Garber JE, Colleoni M, Láng I, et al. Cholesterol, cholesterol-lowering medication use, and breast cancer outcome in the BIG 1-98 study. J Clin Oncol. 2017;35(11):1179-1188.
19. Hsieh LC, Hsieh SL, Ping TN, Huang YC, Lin SJ, Chi HY, et al. Apium graveolens L. alleviates acute lung injury in human A-549 cells by reducing NF-κB and NLRP3 inflammasome signaling. Pharm Biol. 2025;63(1):1-13.
20. Li XY, Yang X, Zhao QD, Han ZP, Liang L, Pan XR, et al. Lipopolysaccharide promotes tumorigenicity of hepatic progenitor cells by promoting proliferation and blocking normal differentiation. Cancer Lett. 2017;386:35-46.
21. Liao M, Yao D, Wu L, Luo C, Wang Z, Zhang J, et al. Targeting the Warburg effect: a revisited perspective from molecular mechanisms to traditional and innovative therapeutic strategies in cancer. Acta Pharm Sin B. 2024;14(3):953-1008.
22. Kwon S, Han SJ, Kim KS. Differential response of MDA-MB-231 breast cancer and MCF10A normal breast cells to cytoskeletal disruption. Oncol Rep. 2023;50(5):200.
23. Sane KM, Mynderse M, LaLonde DT, Dean IS, Wojtkowiak JW, Fouad F, et al. A novel geranylgeranyl transferase inhibitor in combination with lovastatin inhibits proliferation and induces autophagy in STS-26T MPNST cells. J Pharmacol Exp Ther. 2010;333(1):23-33.
24. Sahana J, Corydon TJ, Wehland M, Krüger M, Kopp S, Melnik D, et al. Alterations of growth and focal adhesion molecules in human breast cancer cells exposed to the random positioning machine. Front Cell Dev Biol. 2021;9:672098.
25. Snedec T, Repas J, Lah D, Zemljič Š, Pavlin M. MDA-MB-231 breast cancer cells adapted to anchorage-independent growth reveal senescent-like phenotype and persistent downregulation of PD-L1 expression. Front Oncol. 2025;15:1667308.
26. Murray J, Barbara JAJ, Dunkley SA, Lopez AF, Van Ostade X, Condliffe AM, et al. Regulation of neutrophil apoptosis by tumor necrosis factor-alpha: requirement for TNFR55 and TNFR75 for induction of apoptosis in vitro. Blood. 1997;90(7):2772-2783.
27. Wang B, Song N, Yu T, Zhou L, Zhang H, Duan L, et al. Expression of tumor necrosis factor-alpha-mediated genes predicts recurrence-free survival in lung cancer. PLoS One. 2014;9(12):e115945.
28. Davakis S, Kapelouzou A, Liakakos T, Mpoura M, Stergiou D, Sakellariou S, et al. The role of toll-like receptors in esophageal cancer. Anticancer Res. 2022;42(6):2813-2818.
29. Seol MA, Park JH, Jeong JH, Lyu J, Han SY, Oh SM. Role of TOPK in lipopolysaccharide-induced breast cancer cell migration and invasion. Oncotarget. 2017;8(25):40190-40203.
30. Licarete E, Sesarman A, Banciu M. Exploitation of pleiotropic actions of statins by using tumour-targeted delivery systems. J Microencapsul. 2015;32(7):619-631.
31. Liu S, Li Y, Yuan M, Song Q, Liu M. Correlation between the Warburg effect and progression of triple-negative breast cancer. Front Oncol. 2023;12:1060495.
32. Kali A, Ostapchuk YO, Belyaev NN. TNFα and TGFβ-1 synergistically increase the cancer stem cell properties of MiaPaCa-2 cells. Oncol Lett. 2017;14(4):4647-4658.
33. Lin C, Xin S, Huang X, Zhang F. PTPRA facilitates cancer growth and migration via the TNF-α-mediated PTPRA-NF-κB pathway in MCF-7 breast cancer cells. Oncol Lett. 2020;20(5):131.
34. Politiek FA, Waterham HR. Compromised protein prenylation as pathogenic mechanism in mevalonate kinase deficiency. Front Immunol. 2021;12:724991.
35. Kruys V, Kemmer K, Shakhov A, Jongeneel V, Beutler B. Constitutive activity of the tumor necrosis factor promoter is canceled by the 3' untranslated region in non-macrophage cell lines; a trans-dominant factor overcomes this suppressive effect. Proc Natl Acad Sci U S A. 1992;89(2):673-677.
36. Clayer E, Dalseno D, Kueh A, Lacey D, Tsai M, Arvell EH, et al. Severe impairment of TNF post-transcriptional regulation leads to embryonic death. iScience. 2020;23(11):101726.
37. Crusz SM, Balkwill FR. Inflammation and cancer: advances and new agents. Nat Rev Clin Oncol. 2015;12(10):584-596.